veterinary sciences

MDPI

Article

Effects of Temperature Change on Growth and Maturation, as Well as Tissue Damage and HSP70 Expression in the Black Scraper *Thamnaconus modestus*

Naiqian Zhao [1,2], Yanqing Wu [3,4], Huafeng Zou [4], Jun Zeng [5], Hongkuan Zhang [1,2], Huaiping Zheng [1,2,*] and Wengang Xu [6,*]

[1] Guangdong Provincial Key Laboratory of Marine Biotechnology, Shantou University, Shantou 515063, China; 23nqzhao@stu.edu.cn (N.Z.); hkzhang@stu.edu.cn (H.Z.)
[2] Research Center of Engineering Technology for Subtropical Mariculture of Guangdong Province, Shantou 515063, China
[3] East China Sea Fisheries Research Institute, Chinese Academy of Fishery Sciences, Shanghai 200090, China
[4] College of Fisheries and Life Science, Shanghai Ocean University, Shanghai 201306, China; hfzou@shou.edu.cn
[5] Guangxi Key Laboratory of Marine Environmental Science, Guangxi Academy of Marine Sciences, Guangxi Academy of Sciences, Nanning 530007, China; junzeng@gxas.cn
[6] School of Ocean, Yantai University, Yantai 264005, China
* Correspondence: hpzheng@stu.edu.cn (H.Z.); xugang@ytu.edu.cn (W.X.)

Simple Summary

The black scraper (*Thamnaconus modestus*) is an important marine fish. Adult T. modestus were reared for 4 months at natural water temperature (control group, CG) or constant temperatures of 21 °C (T21) and 24 °C (T24). Heat stress responses were further assessed at 24 °C, 27 °C, and 30 °C. After 120 days, the T21 group exhibited the highest growth rate, gonadosomatic index (GSI), and hepatosomatic index (HSI). Gonads matured in both sexes in the T21 and T24 groups, but not in the CG. Thus, 21 °C and 24 °C accelerated gonadal maturation. In the T24 group, serum E_2 and FSH levels increased significantly in females, and FSH and LH levels rose significantly in males ($p < 0.05$), confirming a strong link between elevated sex hormones and maturation. Heat stress experiments revealed that 27 °C and 30 °C induced gill and liver damage and upregulated HSP70 mRNA and protein expression in gills. Collectively, 21 °C and 24 °C promoted maturation, whereas 27 °C and 30 °C caused tissue injury and altered HSP70 expression.

Abstract

Water temperature critically influences growth and gonadal development in teleosts, yet its effects on adult black scraper (*Thamnaconus modestus*) remain unclear. To address this, 590-day-old *T. modestus* were reared for 4 months under three thermal regimes: natural ambient temperature (control, CG), or constant 21 °C (T21) or 24 °C (T24). Growth indices were measured monthly. Gonadal development was assessed histologically, and serum 17β-estradiol (E_2), testosterone (T), FSH, and LH levels were quantified by ELISA. Heat stress responses were further examined at 24 °C, 27 °C, and 30 °C. Gill and liver tissues were analyzed histologically, and HSP70 mRNA (qRT-PCR) and protein (Western blot) expression were measured. The results showed that after 120 days, growth indices in both sexes from the T21 group were significantly higher than in the control (CG) and T24 groups ($p < 0.05$). The gonadosomatic (GSI) and hepatosomatic (HSI) indices were also highest in the T21 group. In females, oocytes in the T21 and T24 groups reached the secondary and tertiary yolk stages, respectively; in males, testes advanced to the spermatid and spermatozoon stages, respectively. By contrast, CG fish remained in the yolk vesicle and secondary spermatocyte stages, indicating that constant exposure to 21 °C or 24 °C

Check for updates

Academic Editor: M. Enis Yonar

Received: 30 September 2026
Revised: 12 November 2026
Accepted: 13 November 2026
Published: 14 November 2026

Copyright: © 2026 by the authors. Licensee MDPI, Basel, Switzerland. This article is an open access article distributed under the terms and conditions of the Creative Commons Attribution (CC BY) license.

accelerates gonadal maturation in *T. modestus*. At day 120, E_2 and FSH levels in females from T21 and T24 were significantly higher than in CG ($p < 0.05$). In males, FSH and LH levels in T24 exceeded those in CG ($p < 0.05$). These hormonal changes suggest E_2 and FSH drive female maturation, while FSH and LH are key for male maturation. Furthermore, heat stress experiments showed that 27 °C and 30 °C, compared with 24 °C, caused histopathological damage in gill and liver tissues. Concurrently, HSP70 mRNA and protein levels were significantly upregulated in gills ($p < 0.05$), indicating that thermal stress impaired gill and liver integrity and altered HSP70 expression in these tissues. Collectively, compared with the nature temperature, 21 °C and 24 °C supported fast growth and sexual maturation, whereas 27 °C and 30 °C induced significant tissue damage in *T. modestus*.

Keywords: teleosts; high water temperature; 17β-estradiol; testosterone; FSH; LH; HSP70

1. Introduction

In recent years, marine heatwaves have become more frequent and longer-lasting, coinciding with rising global sea surface temperatures [1,2]. As climate change accelerates, the ocean has absorbed over 90% of the Earth's excess heat. Elevated temperatures disrupt fish feeding, growth, and reproduction by altering metabolism and can induce oxidative stress, immune dysfunction, tissue damage, disease, and mortality [3–6]. In China, expanding deep-sea aquaculture and widespread adoption of high-density, intensive farming have made thermal stress a key environmental threat to marine fish health and productivity, jeopardizing the sector's long-term sustainability [7,8]. Mitigating high-temperature stress is thus critical for enhancing resilience and ensuring sustainable development of marine fish aquaculture.

Fish inhabit aquatic environments, and their growth and reproductive processes are tightly coupled with water temperature. Temperature fluctuations regulate gonadal development in Atlantic salmon (*Salmo salar*) [9] and common carp (*Cyprinus carpio*) [10]. Artificially elevated temperatures have been shown to accelerate oocyte maturation and significantly elevate serum E_2 concentrations in red-spotted grouper (*Epinephelus akaara*) [11]. However, comprehensive data on the effects of constant temperature regimes on growth performance, gonadal maturation, and circulating sex hormone profiles, particularly in black scraper (*Thamnaconus modestus*), remain scarce. This knowledge gap directly constrains advances in artificial breeding and seed production technologies for this species.

The black scraper, commonly referred to as the skinless wolf, skinless fish, or horse-faced fish, is a member of the family Monacanthidae (order Tetraodontiformes). It is predominantly distributed in coastal waters adjacent to China, the Korean Peninsula, and Japan. As a warm-water species, it thrives within an optimal temperature range of 21–26 °C [12–14]. Its flesh is highly palatable and commands significant economic value. During the 1960s and 1980s, *T. modestus* ranked as the second most important marine fishery resource in China, surpassed only by the hairtail (*Trichiurus lepturus*) [14]. However, following the 1990s, escalating market demand and intensified wild harvesting, coupled with the persistent failure to develop reliable artificial reproductive technologies, precipitated a steep decline in wild *T. modestus* populations [15]. Although the wild catch increased slightly from 118,909 tons in 2024 to 122,105 tons in 2025, this figure remains substantially lower than historical peaks [16]. To mitigate the shortfall in wild landings, aquaculture production of *T. modestus* has expanded markedly in recent years [17], and the species has emerged as a promising candidate for deep-sea cage culture [18]. Nevertheless, both land-based intensive farming and offshore cage systems depend critically on a consistent and sufficient

supply of high-quality seedlings. Consequently, substantial technological breakthroughs in artificial breeding and larval rearing techniques for *T. modestus* are urgently needed.

Studies indicate that the hypothalamic–pituitary–gonadal (HPG) axis plays a central role in regulating gonadal development and maturation in fish [19,20]. Within this axis, plasma 17β-estradiol (E_2) and testosterone (T), whose synthesis is stimulated by follicle-stimulating hormone (FSH) and luteinizing hormone (LH) secreted from the pituitary, are critically associated with sexual maturation. Sex steroid profiles in teleosts generally conform to patterns observed across vertebrate taxa. For instance, in Arctic charr (*Salvelinus alpinus*) [21], Russian sturgeon (*Acipenser gueldenstaedtii*), and stellate sturgeon (*A. stellatus*) [22], E_2 concentrations remain low during the immature phase but rise markedly upon onset of gonadal maturation. Similarly, in longtooth grouper (*E. bruneus*), female E_2 levels begin to increase in February and reach significantly higher concentrations in April and May, coinciding with active vitellogenesis and oocyte maturation [23]. In contrast, captive dusky groupers (*E. marginatus*) fail to undergo vitellogenesis, likely due to persistently sub-threshold E_2 levels [24]. Furthermore, our previous work demonstrated that elevated E_2 concentrations can directly initiate maturation in juvenile red-spotted groupers, a process potentially mediated by concurrent upregulation of pituitary *Fshβ* and *Lhβ* expression during the mature stage [11].

Research indicates that elevated water temperature exerts significant stress on aquatic organisms, markedly upregulating the expression of heat shock protein 70 (HSP70) [25]. As a highly conserved molecular chaperone in eukaryotes, HSP70 plays a central role in cellular responses to environmental stressors [26]. Under thermal stress, HSP70 is rapidly induced and functions to facilitate proper protein folding and refolding, repair misfolded or damaged proteins, maintain proteostasis, suppress apoptosis, and mitigate oxidative damage [27]. Consequently, HSP70 serves as a critical molecular biomarker for assessing fish physiological responses to heat stress. However, the synergistic regulatory mechanisms linking HSP70 expression to tissue injury remain poorly understood in *T. modestus* [28,29]. To address this knowledge gap, the present study selected *T. modestus* as the model species and conducted controlled-temperature experiments to systematically investigate the effects of water temperature on growth performance, gonadal maturation, and HSP70 expression, thereby elucidating the relationship between thermal stress and HSP70-mediated adaptive responses in this species.

2. Materials and Methods

2.1. Experimental Design

2.1.1. Experimental 1: Growth and Sex Maturation

The experiment was conducted from November 2025 to March 2026 at the East China Sea Fisheries Research Institute, Chinese Academy of Fishery Sciences. Nine circulating culture tanks were established and randomly assigned to three treatment groups: a natural-temperature control group (CG), a 21 °C group (T21), and a 24 °C group (T24), with three replicate tanks per treatment. In the CG, water temperature followed ambient seasonal variation, ranging from 15.3 °C to 18.3 °C throughout the experimental period (Figure 1). Water temperatures in the T21 and T24 groups were maintained at their respective setpoints using calibrated heaters.

A total of 540 healthy *T. modestus* (body weight, 124.58 ± 12.37 g; total length, 18.76 ± 1.21 cm), aged 590 days post-hatching, equally divided into 270 males and 270 females (sex ratio, 1:1), were distributed evenly across nine culture tanks. Each tank contained 60 individuals, 30 males and 30 females. Sex identification was based on a combination of external morphological and physiological characteristics: females were typically larger in overall size, exhibited visibly distended abdomens, and possessed slightly protruding

genital openings; males were generally smaller and displayed elongated dorsal or anal fins and/or elongated snouts [30,31].

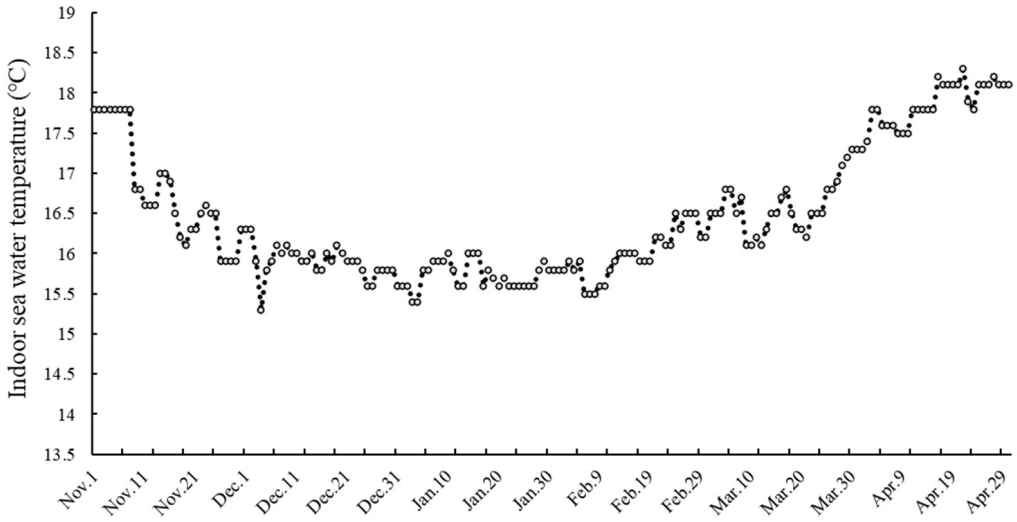


Figure 1. Changes in the indoor seawater temperature during the experiment.

Fish were reared in a recirculating aquaculture system maintained under controlled conditions with continuous 24-h aeration, salinity 28.5–32.5, pH 7.6–8.1, and dissolved oxygen 5.5–6.1 mg/L. Daily water exchange and water quality monitoring were performed in each tank, and fish were fed a commercial compound diet containing 48% crude protein and 14% crude fat twice per day. After each feeding, residual food is promptly removed to prevent any substantial deterioration of water quality. Survival rate remained 100% throughout the experimental period.

2.1.2. Sampling and Measurement of Growth Indices

Sampling was conducted at 0, 30, 60, 90, and 120 days, for a total of five events. During each event, 10 fish, including five males and five females, were randomly collected from each pool. After collection of five samples, ten fish were retained in each tank as a reserve population to mitigate potential mortality during the experiment.

Fish were then anesthetized with 70 mg/L MS-222 (Hangzhou Animal Medicine Factory, Hangzhou, China). The dosages of anesthesia for various teleosts were used as base information [32]. The body weight (BW), total length (TL), and body height were measured. Thereafter, the livers and gonads were dissected, and gonadal weight (GW) and liver weight (LW) were measured. Blood was collected from the caudal vasculature using a heparinized syringe. After centrifugation at 1500× *g* for 15 min, the serum was collected and stored at −80 °C.

Gonads were immediately fixed in Bouin's solution for 24 h, then transferred to 70% ethanol for dehydration and long-term storage prior to histological processing. The gonadosomatic index (GSI, %) and hepatosomatic index (HSI, %) were calculated using the following formulas:

$$GSI = GW/BW \times 100\% \quad (1)$$

$$HSI = LW/BW \times 100\% \quad (2)$$

2.1.3. Experimental 2: Heat Stress Response

The experiment involved three temperature treatment groups of 24 °C, 27 °C, and 30 °C. This experiment was specifically designed to assess the patterns of structural damage progression with increasing temperature; therefore, histological processing and HSP70 expression analysis were not performed on specimens maintained at 21 °C or in the control group. For each temperature treatment, three replicate tanks were established. Fish (body weight: 116.67 ± 16.48 g; total length: 16.88 ± 0.91 cm) were selected and randomly allocated to separate culture tanks, with six individuals per tank. Selected fish exhibited vigorous activity, strong motility, and prompt responsiveness to external stimuli. Their body surfaces were uniformly covered with a clean, transparent mucus layer; no physical injuries, scale loss, or clinical signs of disease were observed.

Feeding and environmental conditions were identical to those used in Experiment 1. After 24 h of thermal acclimation, fish were sampled. All individuals from each tank were humanely anesthetized with 200 mg/L MS-222. Gill and liver tissues were then excised: one set was immediately fixed in Bouin's solution for subsequent histological analysis, while parallel tissue samples were rapidly frozen in liquid nitrogen and stored at −80 °C for downstream molecular and biochemical assays.

2.2. Histological Observation of Gonadal Development

Histological analyses were conducted on gonads (Experiment 1) and on liver and gills (Experiment 2). In Experiment 1, gonads from five males and five females per temperature group (control, 21 °C, and 24 °C) were examined. In Experiment 2, liver and gills from six fish per temperature group (24 °C, 27 °C, and 30 °C) were examined.

The fixed gonadal, gill, and liver tissues were subsequently dehydrated through a graded ethanol series (80%, 85%, 90%, 95%, and 100% v/v). Following dehydration, the tissues were cleared in xylene, embedded in paraffin wax, and serially sectioned at a thickness of approximately 5 μm. Sections were dewaxed in xylene and rehydrated through a descending ethanol series. Thereafter, they were stained with hematoxylin and eosin (H&E), mounted with neutral mounting medium, and examined under an optical microscope (Olympus CX32; Olympus Corporation, Tokyo, Japan). Cell counts in the histological sections were statistically analyzed using ImageJ version 1.54i software. The criterion ultimately adopted for selecting representative images should be that they are visually clear and qualitatively capture the morphological characteristics of the cells.

2.3. Quantification of Serum E_2, T, FSH, and LH Concentrations

The serum concentrations of E_2,T, FSH, and LH were quantified using commercially available enzyme-linked immunosorbent assay (ELISA) Kits (Shanghai Yuduo Biotecnology Co., Ltd., Shanghai, China), specifically the Fish 17β-estradiol (E_2) ELISA Detection Kit, Fish Testosterone (T) ELISA Detection Kit, Fish Follicle-Stimulating Hormone (FSH) ELISA Detection Kit, and Fish Luteinizing Hormone (LH) ELISA Detection Kit, respectively.

The assay protocol followed the procedure described in our previous study [33], with minor modifications. Briefly, the assay was performed as follows: (1) Standard wells received 50 μL of standard solutions at varying concentrations; test sample wells received 40 μL of sample diluent plus 10 μL of test sample; blank control wells contained neither sample nor ELISA reagents. (2) A volume of 100 μL of enzyme-conjugated reagent was added to all wells except the blanks. The plate was then sealed and incubated at 37 °C for 60 min. (3) The concentrated wash buffer was diluted 20-fold with deionized water. After removing the sealing film, the liquid was aspirated from each well, and the wells were gently tapped dry. Each well was then filled with diluted wash buffer, allowed to stand for 30 s, and subsequently aspirated. (4) Steps in (3) were repeated five times.

Following the final wash, 50 µL of chromogenic substrate solution A was added to each well, followed immediately by 50 µL of substrate solution B. The plate was incubated at 37 °C in the dark for 15 min. (5) The reaction was terminated by adding 50 µL of stop solution to each well. (6) Absorbance (optical density, OD) was measured at 450 nm using a microplate reader (Multiskan MK3; Thermo Scientific, Waltham, MA, USA). Plot the standardized sample concentrations along the horizontal (x-) axis and their corresponding OD measurements along the vertical (y-) axis. Employ rigorous linear regression analysis to model the relationship between concentration and OD for the calibration standards, thereby generating a precise, best-fit linear curve. Finally, leverage the derived regression equation, expressed as y = mx + b, to precisely back-calculate the concentration of each unknown sample from its experimentally measured OD value. The intra- and inter-assay coefficients of variation (%CV) were 11.7 and 13.9% for E_2 and 11.9 and 14.1% for T, respectively. The sensitivities of E_2 and T were defined as minimum detection concentrations of less than 1.0 pg/mL and 10 pg/mL, respectively.

2.4. Quantitative Real-Time PCR Analysis for HSP70 mRNA Expression

Total RNA was extracted from gill and liver tissues of individual fish using SparKZol reagent (SparKJade, Jinan, China) and quantified using a NanoDrop 2000 spectrophotometer (Thermo Scientific Inc., Wilmington, DE, USA). First-strand cDNA was synthesized from 1 µg of total RNA using the HiScript III 1st Strand cDNA Synthesis Kit (Vazyme, Nanjing, China), following the manufacturer's instructions. Gene-specific primers for *HSP70* and *Tubulin* were designed based on sequences retrieved from GenBank and are listed in Table 1. Quantitative real-time PCR (qRT-PCR) was performed to measure *HSP70* mRNA levels using TB Green® Premix Ex Taq™ II (Tli RNase H Plus) Kit (Takara Bio Inc., Dalian, China), with *Tubulin* regarded as the endogenous reference gene. Each 10 µL reaction mixture contained 5 µL TB Green® Premix Ex Taq™ II (Tli RNase H Plus), 0.25 µL of each forward and reverse primer (10 pmol/µL), 1 µL diluted cDNA template, and 3.5 µL nuclease-free ddH_2O. Amplification was carried out on a LightCycler 96 Instrument (Roche Diagnostics, Rotkreuz, Switzerland) under the following thermal cycling conditions: initial denaturation at 95 °C for 30 s, followed by 40 cycles of denaturation at 95 °C for 10 s, annealing at 60 °C for 20 s, and extension at 72 °C for 30 s. The ΔCt value obtained at 24 °C was designated as the control and used for normalization.

Table 1. Forward and reverse primers used for quantitative real-time PCR of *Thamnaconus modestus*.

Gene		Sequence (5′–3′)	Accession No.	Amplicon (bp)	Annealing Temperature (°C)	Amplification Efficiency
HSP70	Forward	ccaccatcaaaagcttcagc	PP349927	133	60	0.943
	Reverse	caaagtctcccatctcctgc			62	
Tubulin	Forward	catggccaaaatgagcaagtg	DQ004560	137	62	0.937
	Reverse	caataaaggtcttctgcctgc			62	

2.5. Western Blot for HSP70 Protein Expression

The gill and liver tissues stored at −80 °C were thawed on ice and lysed in RIPA buffer supplemented with protease and phosphatase inhibitors. Total protein was extracted, quantified using the BCA assay, and normalized to equal concentrations. Equal amounts of protein were resolved by SDS-PAGE and electrophoretically transferred onto nitrocellulose membranes. Membranes were blocked with 5% (w/v) non-fat dry milk in TBST (20 mM Tris–HCl, pH 7.4, 150 mM NaCl, 0.1% Tween-20) for 1 h at room temperature. Primary antibodies, mouse monoclonal anti-HSP70 (1:1000; Thermo Fisher Scientific, Fremont, CA, USA) and mouse monoclonal recombinant anti-β-Tubulin (1:2000; Servicebio, Wuhan, China), were diluted in blocking buffer and incubated overnight at 4 °C with

gentle agitation. Following three 10 min washes in TBST, membranes were incubated with horseradish peroxidase (HRP)-conjugated goat anti-mouse IgG (H + L) secondary antibody (1:10,000; ZenBio, Chengdu, China) for 2 h at room temperature. Immunoreactive bands were visualized using enhanced chemiluminescence (ECL) reagent (Wuhan Sanying, Wuhan, China). Chemiluminescent signals were captured using a GelView6000 Pro II imaging system (Guangzhou Biolight Biotechnology Co., Ltd., Guangzhou, China), and band intensities were quantified using ImageJ version 1.54i software. β-Tubulin served as the loading control. The ratio of HSP70 to β-tubulin band intensities measured at 24 °C served as the control and was normalized accordingly.

2.6. Statistical Analysis

All data were analyzed using SPSS 26.0 software (IBM, Armonk, NY, USA). Data are presented as mean ± standard deviation (SD). For comparisons of within-group or between groups involving a single factor, the normality and homoscedasticity of continuous variables were assessed using the Shapiro–Wilk test and Levene's test, respectively. When both assumptions were satisfied, differences between groups or across time points were evaluated using one-way analysis of variance (ANOVA), followed by Tukey's honest significant difference (HSD) post hoc test. For data exhibiting mild deviation from normality, appropriate transformations, such as logarithmic transformation for right-skewed distributions, were applied. If transformation failed to restore normality or if the original data were markedly non-normal, non-parametric alternatives to ANOVA (e.g., the Kruskal–Wallis test) were employed. All statistical tests were two-sided, and differences with $p < 0.05$ were considered statistically significant.

3. Results

3.1. Changes in Growth Indices of Female and Male T. modestus

At the end of the experiment, the BW, GW, and LW of female fish in the T21 group were significantly higher than both their initial values and those of the control group ($p < 0.05$; Table 2). As shown in Figure 2A,B, from day 30 to day 120, GSI and HSI of female fish in the T21 group remained consistently higher than those in all other groups. Specifically, T21 GSI was significantly higher than control at days 60, 90, and 120 ($p < 0.05$) and higher than T24 at days 90 and 120. At day 60, T21 GSI also exceeded that of both T24 and T26. HSI followed a similar trend; at day 120, T21 HSI was significantly higher than T24 ($p < 0.05$).

Table 2. Changes in growth indices of female and male *Thamnaconus modestus* across different temperatures.

Sex	Sampling Time	Group	Body Weight (g)	Total Length (cm)	Body Height (cm)	Gonad (g)	Liver (g)
Female	Start of experiment	—	131.63 ± 11.89 ^{a}	18.35 ± 0.96	6.43 ± 0.96	1.27 ± 0.11 ^{a}	5.69 ± 0.64 ^{a}
	End of experiment	Control	169.35 ± 21.24 ^{a}	21.95 ± 2.48	7.93 ± 1.46	2.96 ± 0.84 ^{a}	12.38 ± 1.79 ^{a}
		21 °C	220.32 ± 25.04 ^{b}	24.74 ± 1.45	8.89 ± 1.78	4.89 ± 0.74 ^{b}	23.52 ± 2.62 ^{b}
		24 °C	194.78 ± 15.11 ^{ab}	23.49 ± 1.69	8.15 ± 1.14	3.43 ± 1.22 ^{ab}	15.37 ± 2.42 ^{ab}
Male	Start of experiment	—	121.72 ± 18.06 ^{A}	20.15 ± 0.91	7.15 ± 1.49	0.78 ± 0.11 ^{A}	4.73 ± 1.01 ^{A}
	End of experiment	Control	148.67 ± 16.48 ^{A}	21.93 ± 1.75	7.82 ± 1.25	2.54 ± 0.38 ^{AB}	11.19 ± 1.32 ^{B}
		21 °C	173.49 ± 25.68 ^{B}	23.93 ± 2.06	8.37 ± 1.84	3.31 ± 0.61 ^{B}	13.13 ± 2.60 ^{B}
		24 °C	164.67 ± 16.32 ^{AB}	23.17 ± 2.65	7.98 ± 1.94	2.69 ± 1.19 ^{AB}	11.79 ± 2.34 ^{B}

Note: The means with different lower-case letters in the female and different capital letters in the male within the same column are significantly different at the 0.05 probability level, with the same lower-case letters or those without letters not showing significant differences at the 0.05 probability level.

The BW of male fish in the T21 group was significantly higher than both the initial value and that of the control group ($p < 0.05$). Similarly, GW in the T21 group exceeded the initial value significantly ($p < 0.05$; Table 2). The GSI of male fish in the T21 group remained

the highest throughout days 30–120: it was significantly higher than the control and T24 groups at day 90, higher than T24 at day 120, and higher than all other treatment groups at day 60 ($p < 0.05$; Figure 2C). At experiment end, the HSI increased significantly in the control, T21, and T24 groups versus their respective baselines ($p < 0.05$; Figure 2D). Overall, both female and male fish showed the most favorable growth indices in the T21 group.

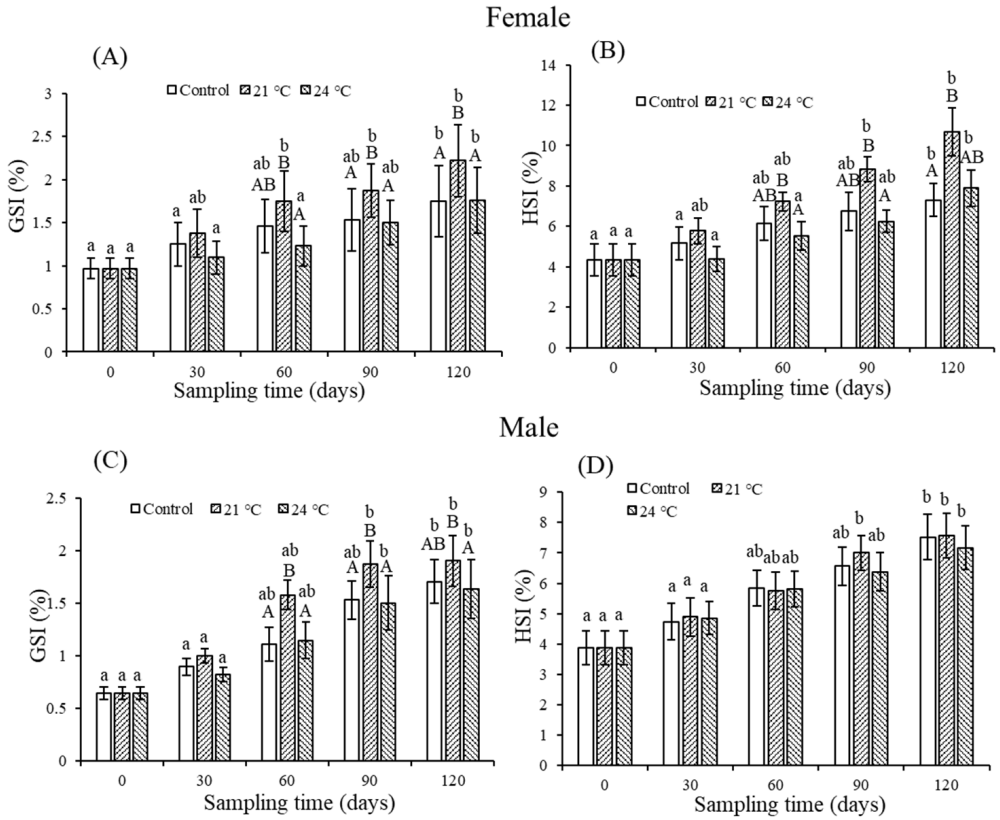


Figure 2. Changes in GSI and HSI of female and male *Thamnaconus modestus* during the experimental period. (**A**,**B**) Female GSI and HSI; (**C**,**D**) male GSI and HSI. Within each group, means sharing different lowercase letters differ significantly ($p < 0.05$); those with the same or no letter do not. Among treatments within each time period, means sharing different uppercase letters differ significantly ($p < 0.05$); those with the same or no letter do not. The same format for statistical presentation has been applied to the other images, where relevant.

3.2. Histological Observations of Gonadal Development in Female and Male T. modestus

Prior to the experiment, oocytes in female fish were predominantly at the yolk vesicle (Yv) stage (Figure 3A), characterized by eosinophilic nuclei and basophilic cytoplasm. In male fish, testes consisted mainly of primary spermatocytes (Ps) (Figure 3B), which were large and spherical, with centrally located basophilic nuclei.

At the conclusion of the experiment, oocytes in the control group remained predominantly at the yolk vesicle (Yv) stage (Figure 3C). The proportional frequency was 100% (Figure 4A). In contrast, in the testes, most germ cells had progressed to the secondary spermatocyte (Ss) stage (Figure 3D), resulting from the meiotic division of primary spermatocytes. Cellular volume decreased relative to baseline, while nuclear basophilia intensified and staining intensity deepened. The proportional frequency was 100% (Figure 4B).

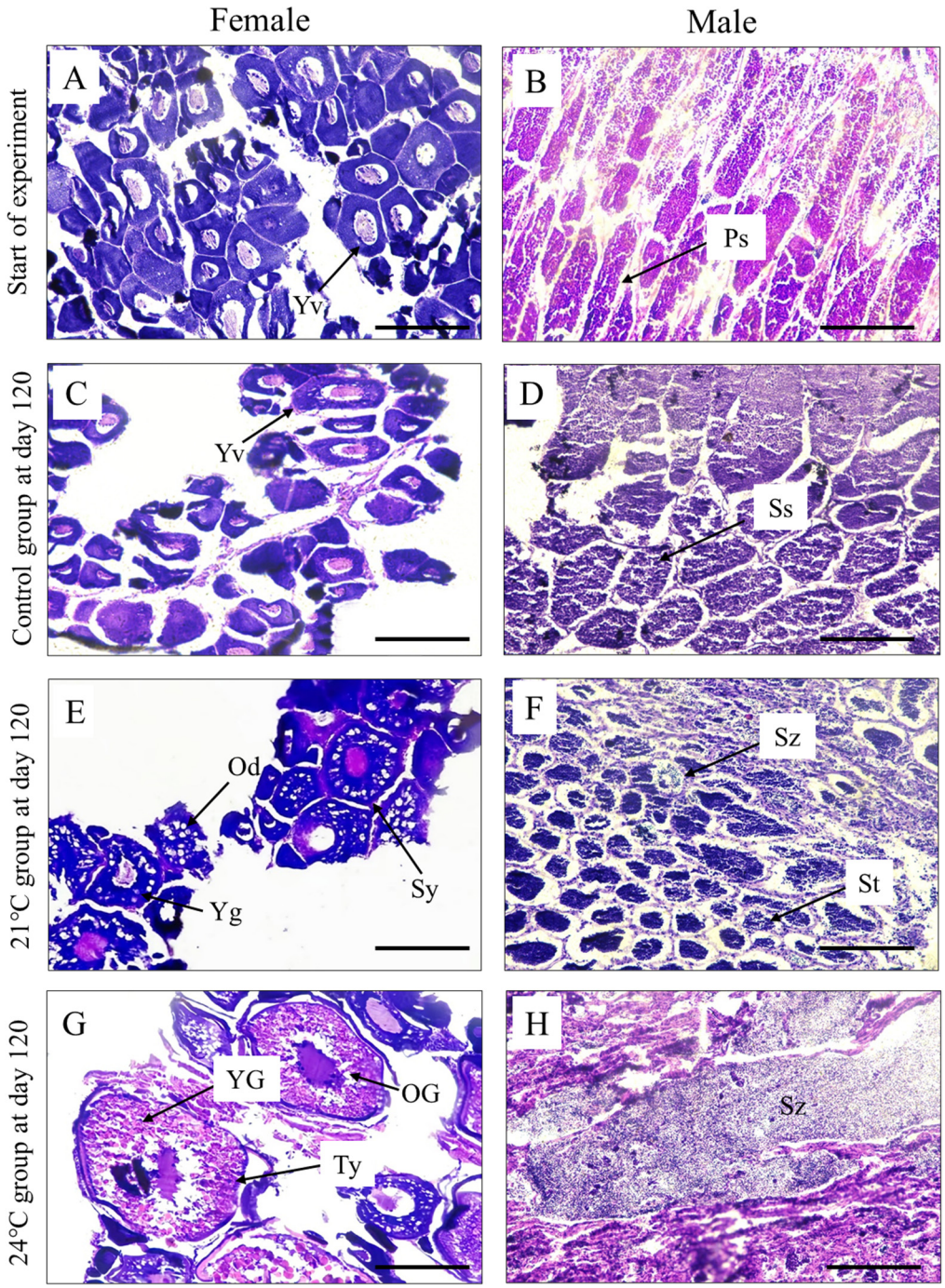


Figure 3. Histological examination of gonadal development in female and male *Thamnaconus modestus* across experimental groups at the start and after 120 days. (**A**,**B**), gonadal development of female and male at start of experiment; (**C**,**D**), gonadal development of female and male in the control group at day 120; (**E**,**F**), gonadal development of female and male in the 21 °C group at day 120; (**G**,**H**), gonadal development of female and male in the 24 °C group at day 120. Femails: Yv, yolk vesicle; Sy, secondary yolk; Ty, tertiary yolk; Yg, yolk granules; Od, oil droplets; YG, yolk globules; OG, oil globules. Males: Ps, primary spermatocyte; Ss, secondary spermatocyte; St, spermatid; Sz, spermatozoon. Scale bar = 100 μm.

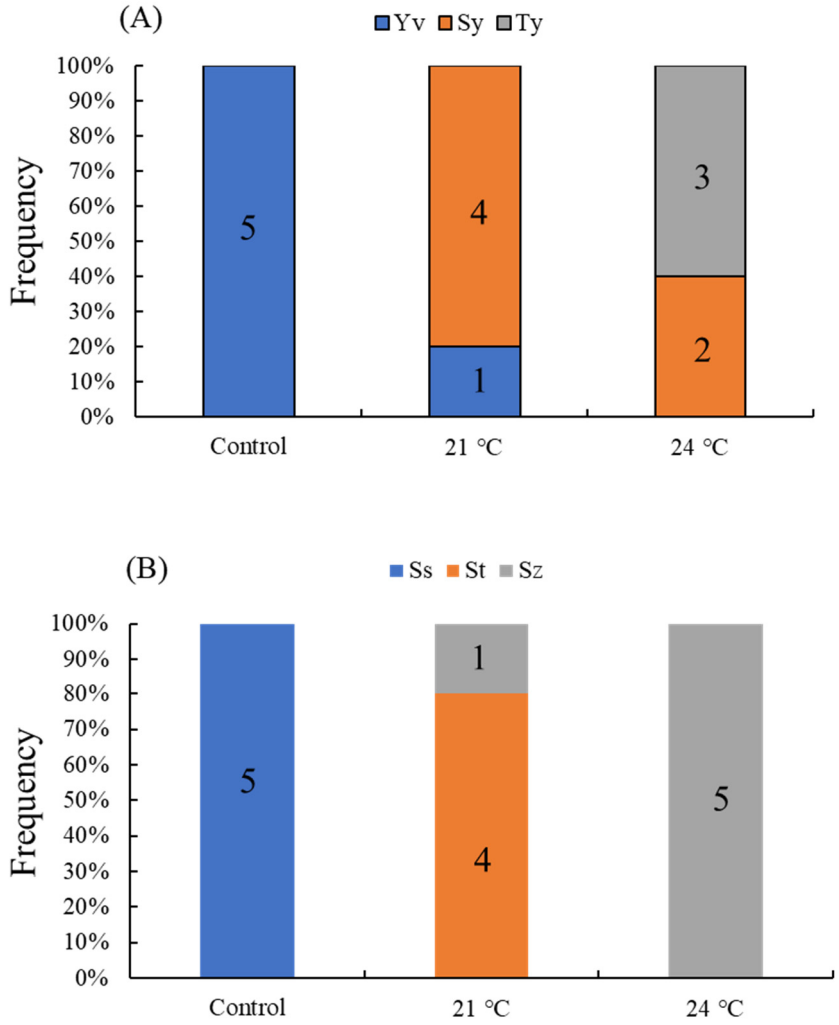


Figure 4. Changes in the proportional frequencies of gonadal developmental stages in females and males across control, 21 °C, and 24 °C treatments. (**A**) Femails: Yv, yolk vesicle; Sy, secondary yolk; Ty, tertiary yolk; (**B**) Males: Ss, secondary spermatocyte; St, spermatid; Sz, spermatozoon.

In the T21 group, oocytes advanced to the secondary yolk globule (Sy) stage (Figure 3E). As cellular volume increased, the nucleolus enlarged. Small yolk granules appeared in the cytoplasm and gradually accumulated from the periphery toward the center, interspersed with a few vacuoles. The proportional frequency was 80% (Figure 4A). Concurrently, most testicular cells, derived from the division of spermatogonia (Ss), progressed to the spermatocyte (St) stage (Figure 3F). Their cellular volume decreased further, and the nuclei became rounder and strongly alkaline. The proportional frequency was 80% (Figure 4B).

In the T24 group, oocytes advanced further to the tertiary yolk globule (Ty) stage (Figure 3G), characterized by progressive fusion of yolk granules into coarse yolk globules and coalescence of small oil droplets into larger oil globules. The proportional frequency was 60% (Figure 4A). Concurrently, testicular cells differentiated into spermatozoa (Sz) (Figure 3H), exhibiting the smallest cellular volume, a spherical morphology, and a strongly basophilic nucleus. The proportional frequency was 100% (Figure 4B).

3.3. Changes in E_2, T, FSH, and LH Levels in Female T. modestus

At the end of the experiment, serum T and LH levels in females increased relative to baseline but showed no significant differences among groups ($p > 0.05$; Figure 5B,D).

In contrast, E_2 and FSH changed significantly over time, indicating clear developmental progression. At day 90, E_2 was significantly higher in the T24 group than in controls ($p < 0.05$; Figure 5A); by day 120, both T21 and T24 groups showed significantly elevated E_2 versus controls and baseline ($p < 0.05$). FSH in the T21 group was significantly higher than in the CG at day 90 ($p < 0.05$; Figure 5C); by day 120, both T21 and T24 groups were significantly higher than the CG and baseline ($p < 0.05$).

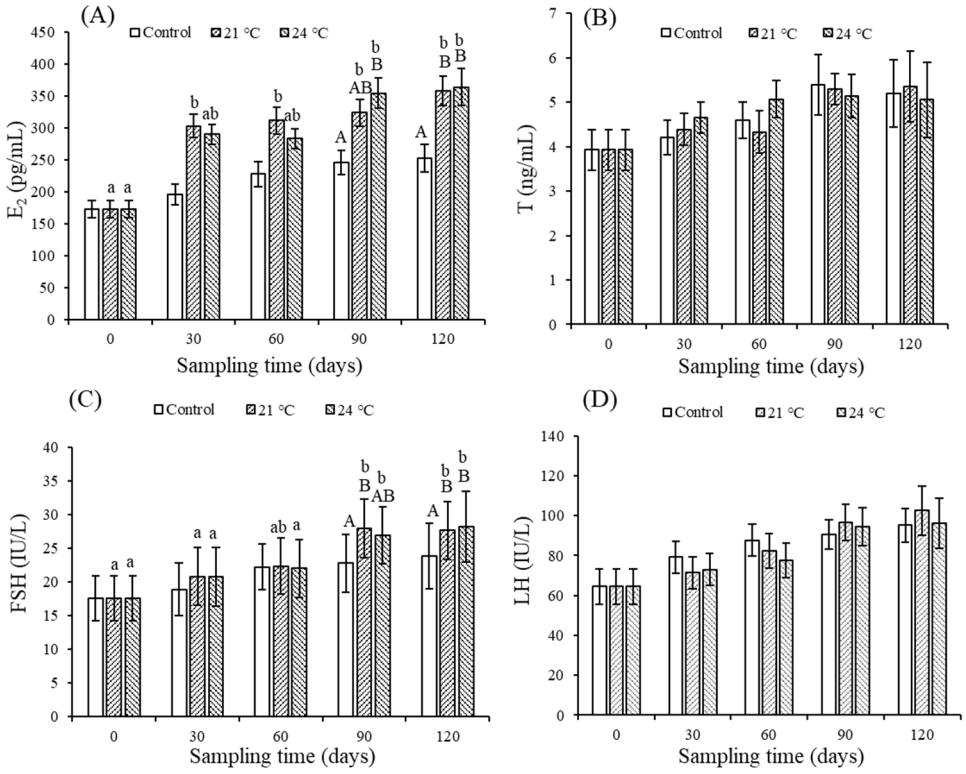


Figure 5. Changes in the serum levels throughout the experimental period in female *Thamnaconus modestus*. (**A**) E_2; (**B**) T; (**C**) FSH; (**D**) LH.

3.4. Changes in E_2, T, FSH, and LH Levels in Male T. modestus

During the experiment, T and E_2 levels did not differ significantly among male fish treatment groups ($p > 0.05$; Figure 6A,B). In contrast, FSH and LH levels changed significantly over time. At day 120, FSH was significantly higher in the T24 group than in controls ($p < 0.05$; Figure 6C), and LH was significantly elevated in both T21 and T24 groups versus controls ($p < 0.05$; Figure 6D).

3.5. Morphological Observation of Gill and Liver Tissues at 24 °C, 27 °C and 30 °C

At 24 °C, gill architecture and axis were well preserved. The primary filaments were regularly aligned, secondary lamellae uniformly distributed, and epithelial layers intact and continuous (Figure 7A). At 27 °C, it showed mild lamellar thickening and focal epithelial hyperplasia, indicating early gill injury (Figure 7B). At 30 °C, severe damage occurred: marked epithelial hyperplasia and tissue enlargement distorted the gill axis; lamellae were thickened, desquamated debris coated filament bases, and inflammatory infiltration was pronounced. Adjacent lamellae fused due to hyperplasia, eliminating interlamellar spacing. Gill lobular vessels were congested, and interstitial edema was evident (Figure 7C).

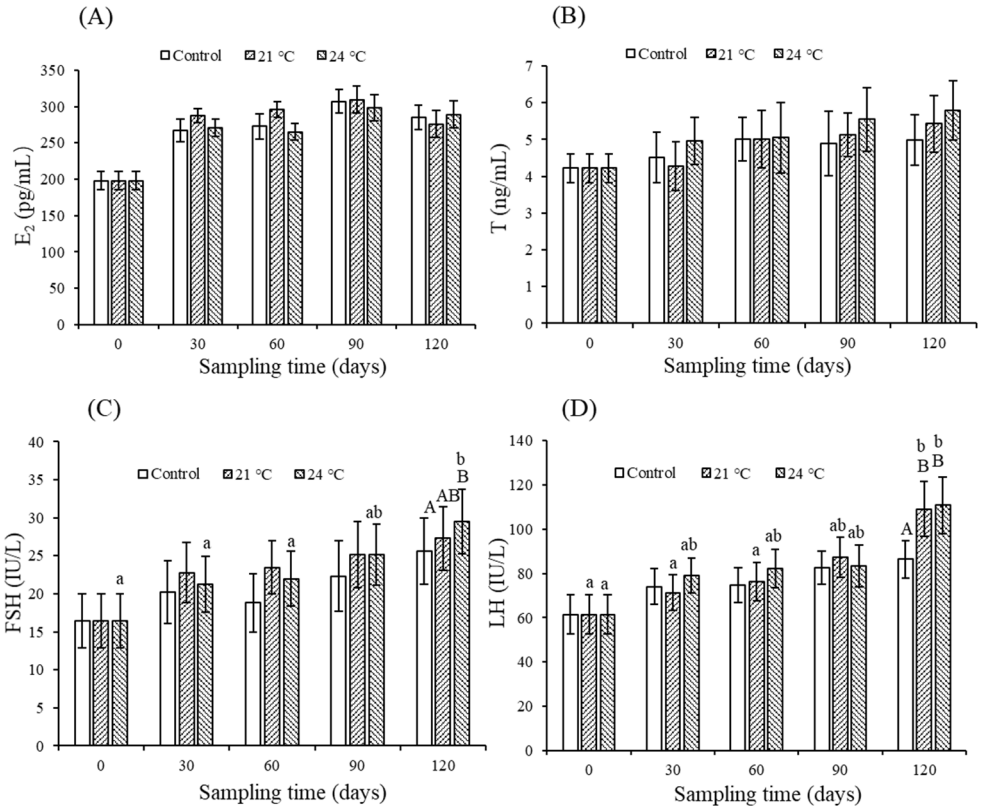


Figure 6. Changes in the serum levels throughout the experimental period in male *Thamnaconus modestus*. (**A**) E_2; (**B**) T; (**C**) FSH; (**D**) LH.

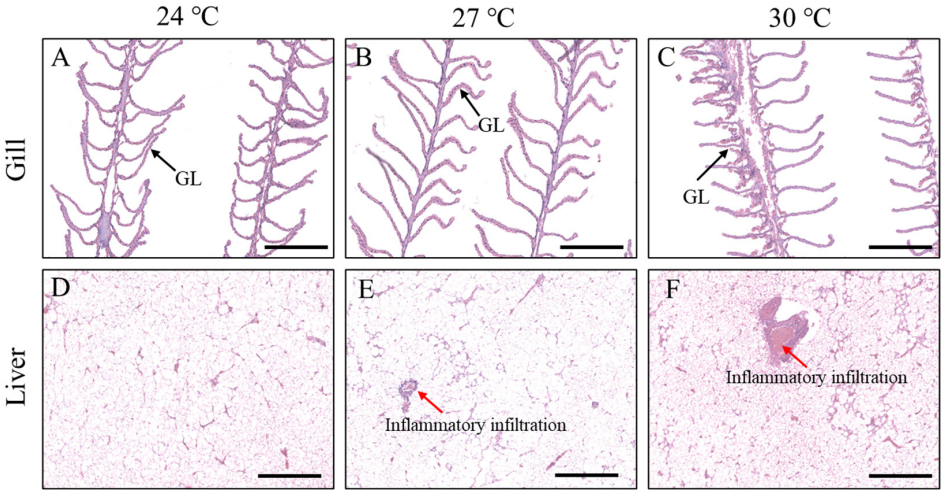


Figure 7. HE staining of gill and liver tissues at different temparatures in *Thamnaconus modestus*. (**A**) Gill; (**B**) Liver. GL, Gill lamellae. Scale bar = 100 μm.

The 24 °C group showed intact hepatic architecture with well-organized hepatocyte plates, uniform cytoplasmic staining, preserved nuclei, and normal sinusoids (Figure 7D). At 27 °C, hepatocellular vacuolization intensified, compressing and displacing nuclei; interplate gaps widened markedly, creating prominent interhepatocytic spaces. Hepatocyte arrangement became disorganized and irregular, with mild inflammatory infiltration (arrow, Figure 7E), indicating greater injury than at 24 °C. At 30 °C, vacuolization worsened and lobular architecture was severely disrupted: hepatocyte plates fragmented and disarrayed; some nuclei showed pyknosis or karyolysis; focal necrosis was evident. A dense

perivascular and/or periportal inflammatory band formed (arrow, Figure 7F), reflecting substantially more severe injury than at 27 °C.

3.6. Relative HSP70 mRNA Expression at 24 °C, 27 °C and 30 °C

The relative *HSP70* mRNA expression in gills increased with temperature, peaking at 27 °C, and was significantly higher than at 24 °C ($p < 0.05$; Figure 8A). In contrast, hepatic *HSP70* mRNA expression decreased with rising temperature, reaching its lowest level at 30 °C, significantly lower than at 24 °C ($p < 0.05$; Figure 8B).

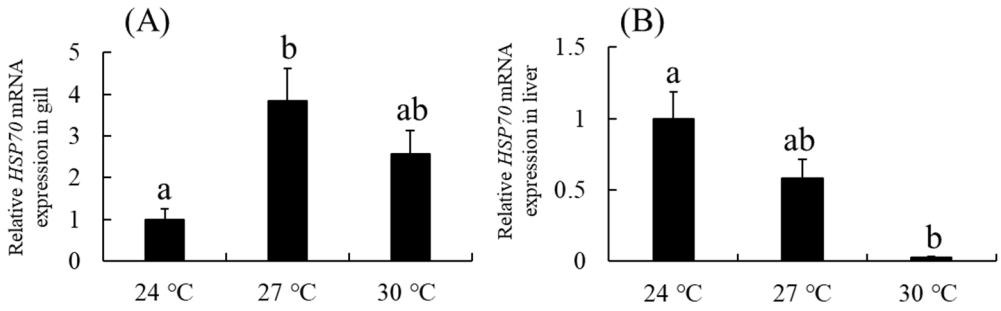


Figure 8. Relative *HSP70* mRNA expression in gill and liver tissues of *Thamnaconus modestus* across temperatures. (**A**) Gill; (**B**) Liver. Means sharing the same lowercase letter are not significantly different ($p > 0.05$); different letters indicate significant differences ($p < 0.05$).

3.7. Relative HSP70 Protein Expression at 24 °C, 27 °C and 30 °C

Western blot analysis of HSP70 and β-tubulin in gill and liver tissues is shown in Figure 9A,C, respectively. In gills, HSP70 protein levels increased progressively with temperature, peaking at 30 °C and remaining significantly higher than at 24 °C ($p < 0.05$; Figure 9B). In the liver, HSP70 expression showed a biphasic pattern, decreasing then increasing, with no significant differences among temperature groups ($p > 0.05$; Figure 9D). The original Western blot bands in gill tissue of HSP70 and β-tubulin were shown in Supplementary Materials (Figures S1 and S2). The original Western blot bands in liver tissue of HSP70 and β-tubulin were shown in Supplementary Materials (Figures S3 and S4).

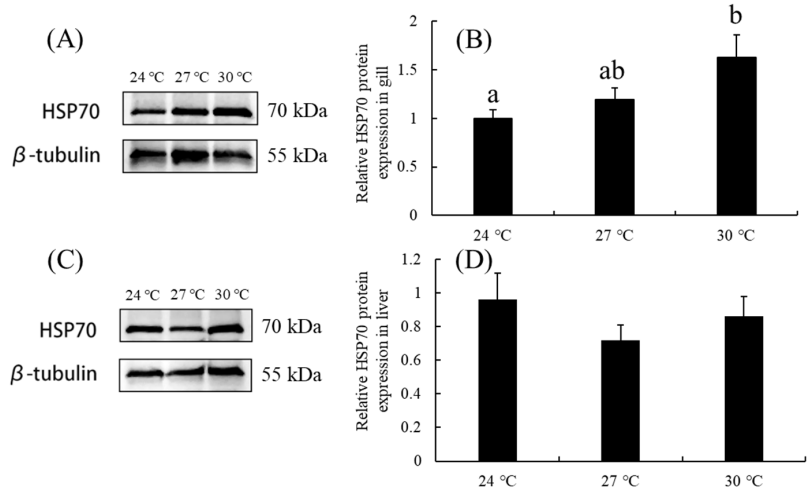


Figure 9. Relative HSP70 protein expression in gill and liver tissues of *Thamnaconus modestus* across temperatures. (**A**) HSP70 Western blot bands with intensity ratio (HSP70/β-tubulin) in gill; (**B**) relative HSP70 expression in gill normalized with control value at 24 °C; (**C**) HSP70 Western blot bands with intensity ratio (HSP70/β-tubulin) in liver; (**D**) relative HSP70 expression in liver normalized with control value at 24 °C.

4. Discussion

4.1. Effects of Water Temperature on Growth of T. modestus

At the end of the experiment, the BW, GSI, and HSI of both male and female *T. modestus* in group T21 were significantly higher than in all other groups, indicating that moderate thermal elevation within the species' physiological range enhances growth and reproductive investment. Water temperature critically regulates metabolic rate and energy allocation during fish development [34]. Within the optimal thermal window, elevated temperature typically increases feeding rate, digestive enzyme activity, and nutrient assimilation efficiency, thereby accelerating somatic growth and supporting greater gonadal investment [35]. For example, 26 °C promoted growth, elevated GSI, and accelerated gonadal development in red-spotted grouper (*E. akaara*) [11]. Juvenile largemouth bronze gudgeon (*Coreius guichenoti*) reared at 26 °C or 30 °C showed significantly higher body length, BW, specific growth rate, weight gain rate, and daily weight gain than those at 22 °C [36]. European sea bass (*Dicentrarchus labrax*) exhibited higher growth rates at 19.5–21 °C than at 18 °C [37]. Collectively, these results support the conclusion that moderate, species-appropriate thermal elevation enhances growth in *T. modestus*. However, the optimal growth performance observed at 21 °C was confined to the experimental period from November 2025 to March 2026. Given the inherent variability and uncertainty of natural water temperatures, further investigation is warranted to determine the robustness and generalizability of this temperature optimum.

4.2. Effects of Water Temperature on Maturation of T. modestus

In this study, gonadal development in the control group progressed more slowly than in both male and female *T. modestus* maintained at 21 °C and 24 °C. Relative to the control group, ovarian development in females advanced to the Sy and Ty stages, whereas testicular development in males reached the St and Sz stages; in contrast, the control group remained at the Yv and Ss stages. These findings indicate that adult *T. modestus* gonads do not undergo spontaneous maturation within four months under natural winter water temperatures in factory-farming conditions, whereas moderate thermal elevation accelerates gonadal maturation. Comparable patterns have been reported in other fish species. Warming promotes gonadal differentiation and growth in *Leporinus friderici* [38] and enhances reproductive probability in the coral reef fish (*Acanthochromis polyacanthus*) [39].

Furthermore, winter warming alleviates ovarian stagnation and promotes oocyte progression from stage II to III, increasing both the GSI and E_2 in *T. modestus* [7]. These findings align with our study, which observed accelerated ovarian development and significantly higher GSI in the T21 and T24 groups of *T. modestus*. However, temperature does not universally enhance gonadal development. Housh et al. [40] reported species-specific effects, ranging from beneficial to detrimental, and even impaired ovarian steroidogenesis in some fish taxa. Thus, thermal effects on gonadal development depend critically on species-specific physiology.

4.3. Effects of E_2 and T on Maturation of T. modestus

In this study, no significant differences in T levels were observed between treatment and control groups in either sex. In contrast, E_2 levels varied significantly. E_2 is a key sex steroid hormone regulating gonadal development and oocyte vitellogenesis in teleosts [41], acting on the liver to stimulate vitellogenin synthesis and secretion, thereby supporting oocyte growth and maturation [42].

In females, serum E_2 concentrations in the T21 and T24 groups were significantly higher than in controls at 90 and 120 days, coinciding with active ovarian vitellogenesis. This E_2 elevation aligned with histological evidence of abundant yolk granules in developing oocytes,

indicating that increased E_2 serves as a pivotal endocrine driver of ovarian development and maturation in *T. modestus*. These findings mirror reports of progressive E_2 increases peaking just before sexual maturity in coho salmon (*Oncorhynchus kisutch*) [43], yellowtail flounder (*Limanda ferruginea*) [44], and leopard grouper (*Mycteroperca rosacea*) [45].

In males, however, no significant differences in serum E_2 were observed across treatment groups. Similarly, E_2 levels remained stable between spawning and non-spawning seasons in male greater amberjack (*Seriola dumerili*) [46] and during the breeding season in male *E. bruneus* [23]. Collectively, these results suggest that male gonadal development relies on steroid hormones via mechanisms distinct from those in females.

4.4. Effects of FSH and LH on Maturation of T. modestus

In this study, plasma FSH levels in female *T. modestus* were significantly higher in the T21 and T24 groups than in controls at both 90 and 120 days post-treatment, suggesting a key role for FSH in ovarian maturation. Similar FSH increases occur during early vitellogenesis in rainbow trout [47], and Planas et al. [48] showed that FSH exerts stage-specific effects on the salmonid ovary. Plasma FSH also rises markedly during vitellogenesis in European sea bass [49]. In mummichog (*Fundulus heteroclitus*), FSH levels are stage-dependent: nearly undetectable (<0.125 ng/mL) post-spawning, low (0.3 ng/mL) during cortical alveoli accumulation, elevated (1.8 ng/mL) in vitellogenesis, and peak (12 ng/mL) at spawning [50]. In greater amberjack (*Seriola dumerili*), pituitary *Fsh* mRNA increases progressively, while plasma Fsh protein surges post-spawning, indicating Fsh activity across multiple ovarian phases, including recovery [51]. Likewise, in salmon, rising plasma FSH coincides with the onset of cortical alveoli accumulation [43]. Collectively, these findings strongly support FSH's critical role in initiating and regulating oocyte maturation. Here, the FSH increase paralleled rising E_2 and progressive yolk deposition, suggesting FSH promotes ovarian maturation in *T. modestus*, at least partly via E_2-mediated pathways. This interpretation aligns with Lubzens et al. [52], who proposed that FSH stimulates follicular E_2 synthesis to promote vitellogenic yolk production. Further studies are needed to clarify the molecular mechanisms underlying FSH-induced E_2 synthesis during ovarian maturation in *T. modestus*.

In male *T. modestus*, circulating FSH and LH were significantly higher in the T24 group than in controls at day 120, coinciding with the histological appearance of spermatozoa, suggesting a functional link between elevated gonadotropins and testicular maturation. Similarly, in rainbow trout, plasma FSH rose ~1 year before spermiation (during late testicular development), while LH increased progressively and peaked just before spermiation [47]. In mummichog, both FSH and LH surged during spawning but remained low or undetectable off-season [50]. Collectively, these findings align with our results and support a conserved role for FSH and LH in regulating male gonadal maturation across teleosts. Further, in European sea bass, FSH rose significantly during mid-spermatogenesis [49], whereas impaired LH secretion during spawning is linked to poor reproductive performance in F1 Senegalese sole (*Solea senegalensis*) males [53]. Together, these data highlight the critical and potentially stage-specific roles of FSH and/or LH in spermatogenesis and testicular maturation in male fish.

4.5. Heat Stress on the Damage of Gill and Liver Tissues of T. modestus

Previous studies show that fish tissue responses to heat stress are organ-specific and linked to organ function, metabolic activity, and exposure conditions [5,6]. In this study, gills exposed to 30 °C showed filament thickening, capillary dilation and congestion, and epithelial cell shedding. Evans et al. [54] attributed such changes, including epithelial proliferation, lamellar fusion, and capillary dilation, to the gills' high metabolic rate and

large surface area exposed to water. Similar histopathological alterations occur in other species: short-term warming impaired immunity and induced gill atrophy in black cusk-eel (*Genypterus maculatus*) [55]; abrupt transfer to 28 °C caused lamellar deformation, swelling, and epithelial fusion in Japanese flounder (*Paralichthys olivaceus*) after 8 h [56]; hybrid sturgeon (*Acipenser baerii*♀× *A. schrenckii* ♂) at 28 °C developed lamellar widening and curling, epithelial edema, and inflammatory cell infiltration into filaments and lamellae [57]; and gill damage worsened with prolonged heat stress in pikeperch (*Sander lucioperca*) [58]. After 12 h at 30 °C, *T. modestus* exhibited marked lamellar curvature, increasing hyperplasia/hypertrophy, intensified cellular vacuolization, and severe edema in flattened epithelial cells [59]. In this study, the gill structural alterations observed in *T. modestus* under elevated temperatures were consistent with those reported in the aforementioned fish species.

Previous studies show that elevated temperatures lead to vacuolization, nuclear condensation, and necrosis in liver [60]. These changes closely match the liver injury morphology observed here. In *T. modestus*, hepatic damage worsens progressively with temperature. At 29 °C, pikeperch showed early injury, hypochromatosis and cytoplasmic vacuolar degeneration immediately (0 h) post-exposure; both intensified over time, peaking at 48 h [61]. Liu et al. reported similar but more severe damage at 30–32 °C (sinusoidal congestion, progressive vacuolation, loss of cellular definition, pyknosis, nucleolysis) and markedly worse lesions at 34 °C (vascular rupture, inflammatory infiltration, extensive vacuolization) [62]. In grass carp (*Ctenopharyngodon idellus*), hyperthermia reduces hepatocyte viability and triggers hepatic oxidative damage [63]. Collectively, heat stress causes temperature- and duration-dependent hepatic injury in fish, with severity increasing across biologically relevant temperatures.

4.6. Effects of Heat Stress on HSP70 mRNA and Protein Expression of T. modestus

This study shows that elevated temperatures (27 °C and 30 °C) significantly upregulate both HSP70 gene transcription and protein expression in gill tissue of *T. modestus*. As a highly conserved molecular chaperone, HSP70 promotes refolding of denatured proteins, prevents aggregation, maintains protein conformational stability under stress, and aids degradation of damaged proteins, thereby supporting cellular homeostasis [25,26,29]. Collectively, these functions underscore HSP70's pivotal role in enhancing cellular resilience to environmental stress. In *T. modestus*, the observed upregulation suggests HSP70 bolsters thermal adaptability via the canonical heat shock response pathway. Consistent with this, substantial HSP70 induction under heat stress has been reported in several teleosts, including yellow croaker (*Larimichthys crocea*) [64], European sea bass [65], rainbow trout [66], and juvenile pearl gentian grouper (*E.fuscoguttatus* × *E.lanceolatus*) [67], where HSP70 is widely used as a key biomarker of thermal tolerance. Notably, HSP70 expression is highly tissue-specific, reflecting complex regulatory mechanisms. As the gill interfaces directly with the environment and mediates gas exchange, ionoregulation, and acid–base balance [54], it is especially suited to detect thermal changes rapidly and mount an early heat shock response. Indeed, in this study, gill tissue showed the earliest and strongest HSP70 upregulation among examined tissues.

In contrast, *HSP70* expression decreased significantly in the liver after 24 h at 30 °C. Similar biphasic responses have been reported in other fish species. In spotted sea bass (*Lateolabrax maculatus*), hepatic *HSP70* mRNA increased at 12 h (28 °C) but declined markedly by 24 h [68]. In Japanese flounder (*Paralichthys olivaceus*), *HSP70* rose significantly at 2 h post-heat stress and dropped substantially by 24 h [69]. In Nile tilapia (*Oreochromis niloticus*), exposure to 35 °C induced rapid *HSP70* upregulation, 2.8- and 2.6-fold higher than controls at 6 h, but levels fell sharply by 24 h [70]. Collectively, these findings reveal a consistent temporal pattern across species that initial HSP70 upregulation followed by downregulation

in liver tissue during prolonged heat stress. As a result, intracellular HSP70 distribution and chaperone function may become disrupted, leading to a progressive decline in its protective efficacy over time. Notably, this study did not measure baseline HSP70 at the 24-h pre-treatment time point. Nevertheless, the observed 24-h post-stress decline aligns with prior reports, suggesting that in *T. modestus*, hepatic HSP70 protection is temporally constrained under sustained heat stress. Further work is needed to characterize HSP70 kinetics during the early phase (<24 h) of thermal challenge.

5. Conclusions

Based on the experimental results, the following conclusions were drawn: (1) *T. modestus* in the T21 group showed the highest growth rate and greatest GSI and HSI indices at experiment end; (2) both sexes in the T21 and T24 groups reached sexual maturity, whereas the control group exhibited delayed gonadal development, indicating that moderate warming accelerates maturation; (3) females in T21 and T24 had significantly higher serum E_2 and FSH levels than controls, suggesting a functional link between these hormonal increases and accelerated maturation; (4) males in T24 showed significantly elevated serum FSH and LH versus controls, implying regulatory roles for both hormones in male maturation; and (5) heat stress induced histopathological alterations in the gills and liver and upregulated both HSP70 mRNA and protein expression in the gills. These results enhance our understanding of the reproductive biology of *T. modestus* and hold significant potential for optimizing artificial reproductive technologies. Furthermore, they provide both a theoretical foundation and practical technical guidance for ripening cultivation, artificial reproduction, and seed production in this species. Further investigation into the regulatory mechanisms governing the HPG axis, particularly dynamic changes in gene expression, is warranted.

Supplementary Materials: The following supporting information can be downloaded at https://www.mdpi.com/article/10.3390/vetsci13111226/s1, Figure S1, Western blot membrane of HSP70 (~70 kDa) protein detected with anti-HSP70 (MA3-006; 1:1000; Thermofisher) antibody in gill; Figure S2, Western blot membrane of β-tubulin (~55 kDa) protein detected with anti-β-tubulin (GB15140-100; 1:2000; Servicebio) antibody in gill; Figure S3, Western blot membrane of HSP70 (~70 kDa) protein detected with anti-HSP70 (MA3-006; 1:1000; Thermofisher) antibody in liver; Figure S4, Western blot membrane of β-tubulin (~55 kDa) protein detected with anti-β-tubulin (GB15140-100; 1:2000; Servicebio) antibody in liver.

Author Contributions: Conceptualization, N.Z.; methodology, H.Z. (Huafeng Zou); software, J.Z.; validation, N.Z.; formal analysis, J.Z. and H.Z. (Hongkuan Zhang); investigation, Y.W.; resources, H.Z. (Huafeng Zou); data curation, N.Z.; writing—original draft preparation, W.X.; writing—review and editing, H.Z. (Hongkuan Zhang) and W.X.; visualization, Y.W.; supervision, H.Z. (Huaiping Zheng); project administration, H.Z. (Huaiping Zheng); funding acquisition, W.X. All authors have read and agreed to the published version of the manuscript.

Funding: This work was partly supported by the Central Public-interest Scientific Institution Basal Research Fund, CAFS (2026TS04), Preparation of a Feasibility Report on the COSCO Shipping Offshore Ecological Aquaculture Farm in Haizhou Bay, Lianyungang (3937-HX-2025), Reform and Development Special Project of the Guangxi Academy of Sciences (2024YGFZ505-901), and Fangchenggang Science and Technology Innovation Development Plan Project (AB23006013) in China.

Institutional Review Board Statement: This study was conducted in accordance with the protocols of the Animal Care and Use Committee of Yantai University, China (Permit Number 20230508); the ethics approval date was on 8 May 2023.

Informed Consent Statement: Informed consent was obtained from all subjects involved in the study.

Data Availability Statement: The data presented in this study are available on request from the corresponding authors due to privacy.

Conflicts of Interest: The authors declare no conflicts of interest.

References

1. Smale, D.A.; Wernberg, T.; Oliver, E.C.J.; Thomsen, M.; Harvey, B.P.; Straub, S.C.; Burrows, M.T.; Alexander, L.V.; Benthuysen, J.A.; Donat, M.G.; et al. Marine heatwaves threaten global biodiversity and ecosystem services. *Nat. Clim. Change* **2019**, *9*, 306–312. [CrossRef]
2. Oliver, E.C.; Donat, M.G.; Burrows, M.T.; Moore, P.J.; Smale, D.A.; Alexander, L.V.; Benthuysen, J.A.; Feng, M.; Gupta, A.S.; Hobday, A.J.; et al. Longer and more frequent marine heatwaves over the past century. *Nat. Commun.* **2018**, *9*, 1324. [CrossRef]
3. Iwama, G.K.; Thomas, P.T.; Forsyth, R.B.; Vijayan, M.M. Heat shock protein expression in fish. *Rev. Fish Biol. Fish.* **1998**, *8*, 35–56. [CrossRef]
4. Basu, N.; Todgham, A.E.; Ackerman, P.A.; Bibeau, M.R.; Nakano, K.; Schulte, P.M.; Iwama, G.K. Heat shock protein genes and their functional significance in fish. *Gene* **2002**, *295*, 173–183. [CrossRef]
5. Madeira, D.; Narciso, L.; Cabral, H.N.; Vinagre, C.; Diniz, M.S. Influence of temperature in thermal and oxidative stress responses in fish. *Comp. Biochem. Physiol. Part A Mol. Integr. Physiol.* **2013**, *166*, 237–243. [CrossRef]
6. Vinagre, C.; Madeira, D.; Narciso, L. Impact of climate change on fish physiology. *Rev. Fish Biol. Fish.* **2012**, *22*, 365–377. [CrossRef]
7. Liu, Y.; Xu, W.G.; Zhang, X.L.; Wang, J.L.; Chen, X.; Yu, X.; Zeng, J.; Wu, Y.Q.; Liu, L.M. The molecular mechanism of ovary development in *Thamnaconus septentrionalis* induced by rising temperature via transcriptomics and metabolomics analysis. *Front. Mar. Sci.* **2025**, *12*, 1556002. [CrossRef]
8. Lushchak, V.I. Environmentally induced oxidative stress in aquatic animals. *Aquat. Toxicol.* **2011**, *101*, 13–30. [CrossRef]
9. Crouse, C.; Davidson, J.; Good, C. The effects of two water temperature regimes on Atlantic salmon (*Salmo salar*) growth performance and maturation in freshwater recirculating aquaculture systems. *Aquaculture* **2022**, *553*, 738063. [CrossRef]
10. Li, Y.; Chen, K.; Gui, B.; Yang, C.; He, L.; Liao, L.; Huang, R. Effect of long-term temperature-controlled rearing on growth traits and sexual maturity of common carp (*Cyprinus carpio*). *Aquaculture* **2024**, *593*, 741271. [CrossRef]
11. Xu, W.G.; Soyano, K.; Manabe, S. High water temperature triggers early sexual maturation in the juvenile red spotted grouper *Epinephelus akaara*: Via regulation of reproduction-related hormones in the brain-pituitary-gonadal axis. *Anim. Reprod. Sci.* **2024**, *268*, 107546. [CrossRef]
12. Mizuno, K.; Shimizu-Yamaguchi, S.; Miura, C.; Miura, T. Method for efficiently obtaining fertilized eggs from the black scraper *Thamnaconus modestus* by natural spawning in captivity. *Fish. Sci.* **2012**, *78*, 1059–1064. [CrossRef]
13. Kim, H.R.; Choi, J.H.; Park, W.G. Vertical distribution and feeding ecology of the black scraper, *Thamnaconus modestus*, in the Southern Sea of Korea. *Turk. J. Fish. Aquat. Sci.* **2013**, *13*, 249–259. [CrossRef]
14. Liu, L.; Zeng, J.; Zhang, Z.; Wang, J.; Mei, W.; Wang, C.; Xu, W.G. Changes in growth, morphology, and levels of digestive enzymes and growth-related hormones in early ontogeny of black scraper, *Thamnaconus modestus*. *Front. Mar. Sci.* **2024**, *11*, 1344844. [CrossRef]
15. Bian, L.; Li, F.H.; Ge, J.L.; Wang, P.F.; Chang, Q.; Zhang, S.N.; Li, J.; Liu, C.; Liu, K.; Liu, X.; et al. Chromosome-level genome assembly of 1. the greenfin horse-faced filefish (*Thamnaconus septentrionalis*) using Oxford Nanopore PromethION sequencing and Hi-C technology. *Mol. Ecol. Resour.* **2020**, *20*, 1069–1079. [CrossRef]
16. Wang, D.; Wu, F.X. *China Fishery Statistical Yearbook*; China Agriculture Press: Beijing, China, 2026.
17. Guan, J.; Ma, Z.; Zheng, Y.; Guan, S.; Li, C.; Liu, H. Breeding and larval rearing of bluefin leatherjacket, *Thamnaconus modestus* (Günther, 1877) under commercial scales. *Int. J. Aquacult.* **2013**, *3*, 55–62. [CrossRef]
18. Mao, X.; Liu, L.; Wang, J.; Liu, Y.; Wu, Y.; Jiang, H. Histological observation on the gonadal development of the parental *Thamnaconus modestus* during early reproductive regulation. *J. Fish. Res.* **2024**, *46*, 11–18. [CrossRef]
19. Maruska, K.P.; Fernald, R.D. Social Regulation of Gene Expression in the Hypothalamic-Pituitary-Gonadal Axis. *Physio* **2011**, *26*, 412–423. [CrossRef]
20. Zohar, Y.; Mylonas, C.C. Endocrine manipulations of spawning in cultured fish: From hormones to genes. *Aquaculture* **2001**, *197*, 99–136. [CrossRef]
21. Frantzen, M.; Jaohnsen, H.K.; Mayer, I. Gonadal development and sex steroids in a female *Arctic charr* broodstock. *J. Fish Biol.* **1997**, *51*, 697–709. [CrossRef]
22. Barannikova, I.A.; Bayunova, L.V.; Semenkova, T.B. Serum levels of testosterone, 11-ketotestosterone and oestradi-ol-17β in three species of sturgeon during gonadal development and final maturation induced by hormonal treatment. *J. Fish Biol.* **2004**, *64*, 1330–1338. [CrossRef]
23. Masuma, S.; Kusunoki, Y.; Aoki, R. Seasonal changes of plasma sex steroids in captive longtooth grouper *Epinephelus bruneus* (Bloch) in subtropical regions. *Aquac. Res.* **2022**, *53*, 1268–1275. [CrossRef]

24. Rodrigues-Filho, J.A.; Araújo, B.C.; Mello, P.H.; Garcia, C.E.O.; Silva, V.F.D.; Li, W.; Levavi-Sivan, B.; Moreira, R.G. Hormonal profile during the reproductive cycle and induced breeding of the dusky grouper *Epinephelus marginatus* (Teleostei: Serranidae) in captivity. *Aquaculture* **2023**, *566*, 739150. [CrossRef]
25. Feder, M.E.; Hofmann, G.E. Heat-shock proteins, molecular chaperones, and the stress response. *Annu. Rev. Physiol.* **1999**, *61*, 243–282. [CrossRef]
26. Sørensen, J.G.; Kristensen, T.N.; Loeschcke, V. The evolutionary and ecological role of heat shock proteins. *Ecol. Lett.* **2003**, *6*, 1025–1037. [CrossRef]
27. Roberts, R.J.; Agius, C.; Saliba, C.; Bossier, P.; Sung, Y.Y. Heat shock proteins in fish and shellfish and their potential role in stress biomarkers. *J. Fish Dis.* **2010**, *33*, 789–801. [CrossRef]
28. Logan, C.A.; Buckley, B.A. Transcriptomic responses to environmental temperature in eurythermal and stenothermal fishes. *J. Exp. Biol.* **2015**, *218*, 1915–1924. [CrossRef]
29. Deane, E.E.; Woo, N.Y.S. Advances and perspectives on the regulation and expression of piscine heat stress proteins. *Rev. Fish Biol. Fish.* **2011**, *21*, 153–185. [CrossRef]
30. Lebeau, B.; Pageau, G. Comparative urogenital morphology and external sex determination in muskellunge, *Esox masquinongy* Mitchill. *Can. J. Zool.* **1989**, *67*, 1053–1060. [CrossRef]
31. Wang, Q.; Fu, S.; Chen, X.; Duan, Y.; Lei, L.; Fan, Y.; Zhou, C. Analysis of Morphological Characteristics of Male and Female *Gymnocypris eckloni* Herzenstein. *Fishes* **2025**, *10*, 399. [CrossRef]
32. Weber, R.A.; Peleteiro, J.B.; García Martín, L.O.; Aldegunde, M. The efficacy of 2-phenoxyethanol, metomidate, clove oil and MS-222 as anaesthetic agents in the Senegalese sole (*Solea senegalensis* Kaup 1858). *Aquaculture* **2009**, *288*, 147–150. [CrossRef]
33. Xu, W.G.; Liu, Y.; Wang, J.L.; Yang, P.; Wu, Y.Q.; Liu, L.M. Changes in gonadal sex differentiation, digestive enzymes, and growth-related hormone contents in the larval and juvenile black scraper, *Thamnaconus modestus*. *Biology* **2025**, *14*, 1385. [CrossRef]
34. Pörtner, H.O.; Berdal, B.; Blust, R.; Brix, O.; Colosimo, A.; De Wachter, B.; Giuliani, A.; Johansen, T.; Fischer, T.; Knust, R.; et al. Climate induced temperature effects on growth performance, fecundity and recruitment in marine fish: Developing a hypothesis for cause and effect relationships in Atlantic cod (*Gadus morhua*) and common eelpout (*Zoarces viviparus*). *Cont. Shelf Res.* **2001**, *21*, 1975–1997. [CrossRef]
35. Canosa, L.F.; Bertucci, J.I. The effect of environmental stressors on growth in fish and its endocrine control. *Front. Endocrinol.* **2023**, *14*, 1109461. [CrossRef]
36. Li, X.; Wu, X.; Li, X.; Zhu, T.; Zhu, Y.; Chen, Y.; Yang, D. Effects of water temperature on growth performance, digestive enzymes activities, and serum indices of juvenile *Coreius guichenoti*. *J. Therm. Biol.* **2023**, *115*, 103595. [CrossRef]
37. Besson, M.; Vandeputte, M.; Van Arendonk, J.A.M. Influence of water temperature on the economic value of growth rate in fish farming: The case of sea bass (*Dicentrarchus labrax*) cage farming in the Mediterranean. *Aquaculture* **2016**, *462*, 47–55. [CrossRef]
38. Souza, T.G.; Abreu, M.R.; Kuradomi, R.Y.; Batlouni, S.R. Effect of temperature on gonadal differentiation and growth of *Leporinus friderici*. *Anim. Reprod.* **2024**, *21*, e20230158. [CrossRef]
39. Spinks, R.K.; Bonzi, L.C.; Ravasi, T.; Munday, P.L.; Donelson, J.M. Sex- and time-specific parental effects of warming on reproduction and offspring quality in a coral reef fish. *Evol. Appl.* **2021**, *14*, 1145–1158. [CrossRef]
40. Housh, M.J.; Telish, J.; Forsgren, K.L.; Lema, S.C. Fluctuating and stable high temperatures differentially affect reproductive endocrinology of female pupfish. *Integr. Org. Biol.* **2024**, *6*, obae003. [CrossRef]
41. Kazeto, Y.; Tosaka, R.; Matsubara, H.; Ijiri, S.; Adachi, S. Ovarian steroidogenesis and the role of sex steroid hormones on ovarian growth and maturation of the *Japanese eel*. *J. Steroid. Biochem. Mol. Biol.* **2011**, *127*, 149–154. [CrossRef]
42. Sullivan, C.V.; Yilmaz, O. Vitellogenesis and yolk proteins, fish. *Encycl. Reprod.* **2018**, *6*, 266–277. [CrossRef]
43. Campbell, B.; Dickey, J.; Beckman, B.; Young, G.; Pierce, A.; Fukada, H. Previtellogenic oocyte growth in salmon: Relationships among body growth, plasma insulin-like growth factor-1, estradiol-17beta, follicle-stimulating hormone and expression of ovarian genes for insulin-like growth factors, steroidogenic-acute regulatory protein and receptors for gonadotropins, growth hormone, and somatolactin. *Biol. Reprod.* **2006**, *75*, 34–44. [CrossRef]
44. Manning, A.J.; Burton, M.P.M.; Crim, L.W. The timing of puberty in cultured female yellowtail flounder, *Limanda ferruginea* (Storer): Oogenesis and sex steroid production in vivo and in vitro. *Aquaculture* **2008**, *279*, 188–196. [CrossRef]
45. Maldonado-García, M.; Gracia-López, V.; Kiewek-Martínez, M.; Carrillo, M.; Zanuy, S. Reproductive cycle of leopard grouper *Mycteroperca rosacea* held in captivity: Relationship between gonad development and sex steroid concentration. *Lat. Am. J. Aquat. Res.* **2018**, *46*, 83–90. [CrossRef]
46. Aoki, R.; Chuda, H.; Washio, Y. Sex discrimination of cultured greater amberjack *Seriola dumerili* using steroid hormones. *Fish. Sci.* **2020**, *86*, 57–64. [CrossRef]
47. Prat, F.; Sumpter, J.P.; Tyler, C.R.; Graham, C.H.; Watson, J.D.; Blumenfeld, A.J.; Pang, S.C. Validation of radioimmunoassays for two salmon gonadotropins (GTH I and GTH II) and their plasma concentrations throughout the reproductive cycle in male and female rainbow trout (*Oncorhynchus mykiss*). *Biol. Reprod.* **1996**, *54*, 1375–1382. [CrossRef]

48. Planas, J.V.; Athos, J.; Goetz, F.W.; Swanson, P. Regulation of ovarian steroidogenesis in vitro by follicle-stimulating hormone and luteinizing hormone during sexual maturation in salmonid fish. *Biol. Reprod.* **2000**, *62*, 1262–1269. [CrossRef]
49. Molés, G.; Rocha, A.; Espigares, F.; Gómez Peris, A.; Carrillo, M.; Zanuy, S. FSH plasma levels during testicular recrudescence of precocious and non precocious male European sea bass using a newly developed species specific enzyme-linked immunosorbent assay (ELISA). In Proceedings of the 9th International Symposium on Reproductive Physiology of Fish, Cochin, India, 9–14 August 2011. [CrossRef]
50. Shimizu, A.; Ohkubo, M.; Hamaguchi, M. Development of non-competitive enzyme-linked immunosorbent assays for mummichog *Fundulus heteroclitus* gonadotropins–examining seasonal variations in plasma FSH and LH levels in both sexes. *General. Comp. Endocrinol.* **2012**, *178*, 463–469. [CrossRef]
51. Nyuji, M.; Kazeto, Y.; Izumida, D.; Tani, K.; Suzuki, H.; Hamada, K.; Mekuchi, M.; Gen, K.; Soyano, K.; Okuzawa, K. Greater amberjack Fsh, Lh, and their receptors: Plasma and mRNA profiles during ovarian development. *General. Comp. Endocrinol.* **2016**, *225*, 224–234. [CrossRef]
52. Lubzens, E.; Young, G.; Bobe, J.; Cerdà, J. Oogenesis in teleosts: How fish eggs are formed. *Gen. Comp. Endocr.* **2010**, *165*, 367–389. [CrossRef]
53. Chauvigné, F.; Fatsini, E.; Duncan, N.; Ollé, J.; Zanuy, S.; Gómez, A.; Cerdà, J. Plasma levels of follicle-stimulating and luteinizing hormones during the reproductive cycle of wild and cultured Senegalese sole (*Solea senegalensis*). *Comp. Biochem. Physiol. Part A Mol. Integr. Physiol.* **2016**, *191*, 35–43. [CrossRef]
54. Evans, D.H.; Piermarini, P.M.; Choe, K.P. The multifunctional fish gill: Dominant site of gas exchange, osmoregulation, acid–base regulation, and excretion of nitrogenous waste. *Physiol. Rev.* **2005**, *85*, 97–177. [CrossRef]
55. Becerra, S.; Arriagada-Solimano, M.; Escobar-Aguirre, S.; Palomino, J.; Aedo, J.; Estrada, J.M.; Barra-Valdebenito, V.; Zuloaga, R.; Valdes, J.A.; Dettleff, P. High temperature induces oxidative damage, immune modulation, and atrophy in the gills and skeletal muscle of the teleost fish black cusk-eel (*Genypterus maculatus*). *Dev. Comp. Immunol.* **2025**, *164*, 105332. [CrossRef]
56. Yan, W.; Qiao, Y.; He, J.; Qu, J.; Liu, Y.; Zhang, Q.; Wang, X. Molecular Mechanism Based on Histopathology, Antioxidant System and Transcriptomic Profiles in Heat Stress Response in the Gills of Japanese Flounder. *Int. J. Mol. Sci.* **2022**, *23*, 3286. [CrossRef]
57. Yang, S.; Li, D.; Gao, Y.; Wei, Z.; Xiong, Y.; Liu, Y.; Yi, S.; Lyu, X.; Xi, D.; Li, Y.; et al. Heat stress triggers gill damage in hybrid sturgeon (*A. baerii*♀× *A. schrenckii*♂) via synergistic effects on apoptosis, microbial dysbiosis, physical barrier dysfunction, and inflammatory response. *Aquaculture* **2026**, *615*, 743668. [CrossRef]
58. Chen, Y.; Liu, E.; Li, C.; Pan, C.; Zhao, X.; Wang, Y.; Ling, Q. Effects of heat stress on histopathology, antioxidant enzymes, and transcriptomic profiles in gills of pikeperch *Sander lucioperca*. *Aquaculture* **2021**, *534*, 736277. [CrossRef]
59. Chen, Y.; Chen, S.Q.; Zhang, B.; Zheng, Z.J.; Zhang, Y.A.; Chang, Q.; Bian, L. Effects of acute high-temperature on gill tissue structure, serum biochemical indices, antioxidant capacity and liver transcriptomics of *Thamnaconus septentrionalis*. *J. Therm. Biol.* **2025**, *129*, 104098. [CrossRef]
60. Birnie-Gauvin, K.; Costantini, D.; Cooke, S.J.; Willmore, W.G. A comparative review of oxidative stress in fish. *Comp. Biochem. Physiol. Part A Mol. Integr. Physiol.* **2017**, *203*, 94–104.
61. Wang, Y.; Li, C.; Pan, C.; Liu, E.; Zhao, X.; Ling, Q. Alterations to transcriptomic profile, histopathology, and oxidative stress in liver of pikeperch (*Sander lucioperca*) under heat stress. *Fish Shellfish Immunol.* **2019**, *95*, 659–669. [CrossRef]
62. Liu, E.; Zhao, X.; Li, C.; Wang, Y.; Li, L.; Zhu, H.; Ling, Q. Effects of acute heat stress on liver damage, apoptosis and inflammation of pikeperch (*Sander lucioperca*). *J. Therm. Biol.* **2022**, *106*, 103251. [CrossRef]
63. Cui, Y.; Liu, B.; Xie, J.; Xu, P.; Habte-Tsion, H.M.; Zhang, Y. Effect of heat stress and recovery on viability, oxidative damage, and heat shock protein expression in hepatic cells of grass carp (*Ctenopharyngodon idellus*). *Fish Physiol. Biochem.* **2014**, *40*, 721–729. [CrossRef]
64. Qian, B.; Xue, L. Liver transcriptome sequencing and de novo annotation of the large yellow croaker (*Larimichthy crocea*) under heat and cold stress. *Mar. Genom.* **2016**, *25*, 95–102. [CrossRef]
65. Enes, P.; Panserat, S.; Kaushik, S.; Oliva-Teles, A. Rapid metabolic adaptation in European sea bass (*Dicentrarchus labrax*) juveniles fed different carbohydrate sources after heat shock stress. *Comp. Biochem. Physiol. Part A Mol. Integr. Physiol.* **2006**, *145*, 73–81. [CrossRef]
66. Huang, J.; Li, Y.; Liu, Z.; Kang, Y.; Wang, J. Transcriptomic responses to heat stress in rainbow trout *Oncorhynchus mykiss* head kidney. *Fish Shellfish. Immun.* **2018**, *82*, 32–40. [CrossRef]
67. Alatwinusa Yohana, M.; Gyan, W.R.; Yang, Q.; Tan, B.; Lin, H.; Yi, Y.; Chi, S. Dietary L-carnitine supplementation for heat stressed juvenile pearl gentian grouper (*Epinephelusllanolatus* (*Epinepheluso*♂× *Epinephelusfuscoguttatus*♀): Effects on the antioxidant enzyme, survival, and gene expression. *Aquacult. Rep.* **2023**, *29*, 101524. [CrossRef]
68. Shin, M.K.; Park, H.R.; Yeo, W.J.; Han, K.N. Effects of thermal stress on the mRNA expression of SOD, HSP90, and HSP70 in the spotted sea bass (*Lateolabrax maculatus*). *Ocean Sci. J.* **2018**, *53*, 43–52. [CrossRef]

69. Liu, Y.; Ma, D.; Xiao, Z.; Xu, S.; Wang, Y.; Wang, Y.; Xiao, Y.; Song, Z.; Teng, Z.; Liu, Q.; et al. Histological change and heat shock protein 70 expression in different tissues of Japanese flounder Paralichthys olivaceus in response to elevated temperature. *Chin. J. Ocean. Limnol.* **2015**, *33*, 11–19. [CrossRef]
70. Qiang, J.; Yang, H.; Wang, H.; Xu, P.; He, J. The effect of acute temperature stress on biochemical indices and expression of liver Hsp70 mRNA in GIFT Nile tilapia juveniles (*Oreochromis niloticus*). *Oceanol. Limnol. Sin.* **2012**, *43*, 943–953. [CrossRef]

Disclaimer/Publisher's Note: The statements, opinions and data contained in all publications are solely those of the individual author(s) and contributor(s) and not of MDPI and/or the editor(s). MDPI and/or the editor(s) disclaim responsibility for any injury to people or property resulting from any ideas, methods, instructions or products referred to in the content.